

Observation of the waveform of accumulated photon echoes in a dye-doped polymer film by use of an interferometer

Takuya Yoda, Takao Fuji, Toshiaki Hattori, and Hiroki Nakatsuka

Institute of Applied Physics, University of Tsukuba, Tsukuba, Ibaraki 305-8573, Japan

Received March 16, 1999

We used a Michelson-type interferometer to observe the waveform of the accumulated photon echoes in a 3,3'-diethylthiatricarbocyanine iodide-doped poly(vinyl alcohol) film. By Fourier analysis of the measured interferograms we obtained the shapes of the burned population grating and the phase grating in the sample. From the frequency distribution of the dye molecules, that is efficient for persistent spectral hole burning, we estimated the inhomogeneous frequency distribution of the 0-0 transition from S_0 to S_1 levels of the dye molecules in the poly(vinyl alcohol) film. © 1999 Optical Society of America [S0740-3224(99)00210-6]

OCIS codes: 120.0120, 300.0300, 120.5050, 190.4380, 300.6500, 320.7150.

1. INTRODUCTION

Photon echoes are a kind of nonlinear coherent transient phenomenon and are classified as two-pulse echoes, three-pulse echoes, and accumulated echoes, depending on the number of excitation pulses.¹ The key feature of photon echoes is that an echo pulse is emitted at a time τ_1 after the last excitation pulse, where τ_1 is the time separation between the first and the second excitation pulses. This phenomenon is usually described by use of a density matrix or a Bloch vector.

After the first excitation pulse, the polarization of each molecule in a sample starts precession with its own eigenfrequency, and the macroscopic polarization decays with an inhomogeneous phase decay time T_2^* that is the inverse of the inhomogeneous width of the sample while the sample is emitting a free-induction-decay (FID) signal. The second excitation pulse excites the molecule, depending on the relative phase between the polarization of the molecule and the excitation light pulse. Therefore the excited-state population after the second pulse depends on the eigenfrequency of the polarization, and the population distribution has a sinusoidal modulation in the frequency domain. The modulated population distribution, with a period that is equal to the inverse of the time separation τ_1 between the first and the second excitation pulses, is called a population grating. If the sample is irradiated by the third pulse after the second pulse, a FID signal is emitted from the sample with a population grating as a linear response to the third pulse. In this FID signal there is a pulse that is emitted at a time τ_1 after the third pulse, and it is called the three-pulse photon echo. The two-pulse photon echoes can be considered a special case of three-pulse photon echoes in which the second and the third pulses are unified. On the other hand, if two-pulse excitation with the same pulse separation and the same phase relation occurs many times within the population decay time T_1 , the population grating accumulates and the depth of the modulation increases.

From the accumulated population grating we can expect a large photon-echo signal, even when small-peak-power lasers such as cw mode-locked lasers are used. This type of photon echo is called an accumulated photon echo and was demonstrated by Hesselink and Wiersma in 1979.²

From the dependence of the echo intensity on the time separations between excitation pulses we can obtain the homogeneous phase decay time T_2 and the population decay time T_1 .^{1,2} In recent years, however, phase-sensitive pulse-shape measurements were introduced to facilitate the discussion of the ultrafast dynamics of semiconductors and liquids in more detail.³⁻⁷

In the linear regime, the deformation of a light pulse by its passage through a sample can be observed precisely by use of a Michelson-type interferometer with a broad-spectrum light source.⁸⁻¹⁰ Because the photon echoes can be considered the FID signal induced by the last excitation pulse in the sample with a population grating, the interferometric method can be directly applied to observation of the detailed echo pulse shape and to analysis of the burned population grating.

In this paper we present an observation of the pulse shape of accumulated photon echoes in a dye-doped polymer film and make a detailed analysis of the burned population grating and the phase grating. The relation between the burning efficiency of the population grating and the inhomogeneous frequency distribution of the 0-0 transition from S_0 to S_1 levels of the doped dye molecules is also discussed.

2. EXPERIMENTAL SYSTEM

A schematic diagram of the experiment is shown in Fig. 1. The system is composed of two Michelson interferometers; the first one, which is surrounded by a dashed box in the figure, is used for the beam of a train of two excitation pulses to create the population grating in the sample. The second Michelson interferometer is used for

the beam of the last excitation pulse to induce a photon echo pulse and for the reference pulse to interfere with the echo pulse. We obtain the interferogram by scanning the path length or the delay time τ_2 of the signal arm of the second Michelson interferometer. The excitation light is a homemade cw mode-locked Ti:sapphire laser pumped by the second harmonic of a Nd:YVO₄ laser (Spectra-Physics, Millennia), which is pumped by diode lasers. The pulse width and the repetition frequency of the Ti:sapphire laser are 30 fs and 100 MHz, respectively. The time separation τ_1 and thus the phase relation between the two excitation pulses formed by the first Michelson interferometer are locked by the phase-lock loop shown in Fig. 1.¹¹ Here the path length of one arm of the first Michelson interferometer is modulated by a piezoelectric actuator at $f_1 = 5$ kHz with an amplitude of a fraction of the wavelength of light, and the rectified output from the lock-in amplifier is fed into the actuator together with the sinusoidal voltage at f_1 . A narrow-bandpass monochromator is inserted to produce clear interference for phase locking, even at large τ_1 .

The reference arm's path length in the second Michelson interferometer is modulated at $f_2 = 1$ kHz with an amplitude of ~ 250 nm for phase-sensitive lock-in detection of the interferogram. We obtain the autocorrelation interferogram,

$$C_A(\tau) = \langle E_{in}^*(t)E_{in}(t + \tau) \rangle, \quad (1)$$

of the incident mode-locked Ti:sapphire laser light by taking away the sample and scanning the signal-arm path length of the second Michelson interferometer with a stepping motor. The path-length difference of the second Michelson interferometer is calibrated by the autocorrelation interferogram of a He-Ne laser, which is taken simultaneously. In the linear regime the output electric field $E_{out}(t)$ from the sample is written as

$$E_{out}(t) = \int_{-\infty}^t dt' h(t - t')E_{in}(t'), \quad (2)$$

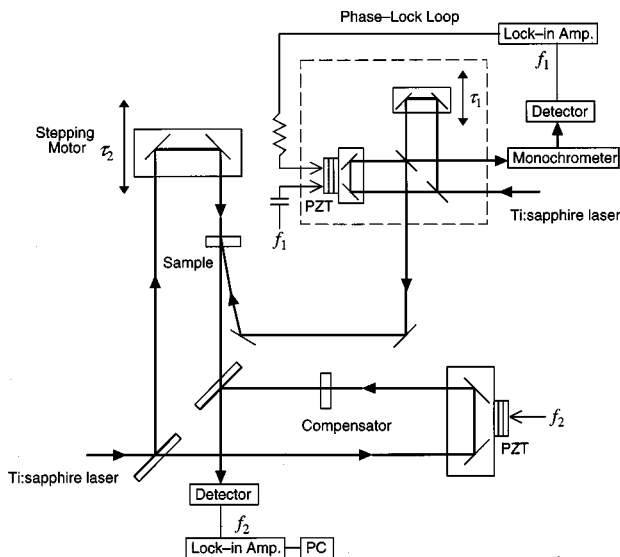


Fig. 1. Schematic diagram of the experiment: PZT's, piezoelectric transducers.

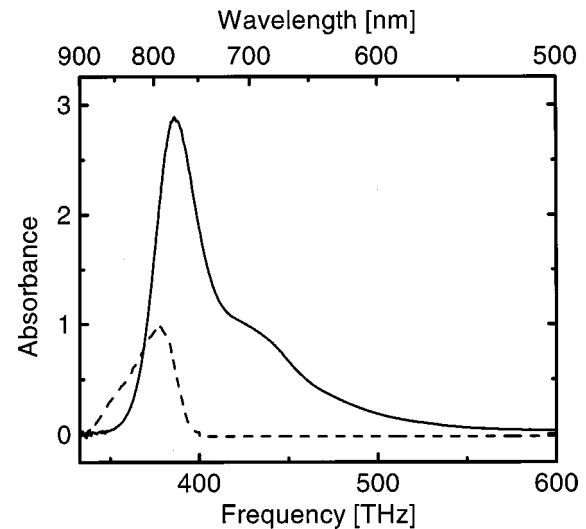


Fig. 2. Absorption spectra of the DTTCI-doped PVA film (solid curve) and the cw mode-locked Ti:sapphire laser (dashed curve).

where $h(t)$ is the impulse-response function of the sample. We obtain the cross-correlation interferogram,

$$C_C(\tau) = \langle E_{in}^*(t)E_{out}(t + \tau) \rangle, \quad (3)$$

between the input field $E_{in}(t)$ and the output field $E_{out}(t)$ by setting the sample in the signal arm of the second Michelson interferometer and scanning the path length of the signal arm. Inserting Eq. (2) into Eq. (3), we obtain

$$C_C(\tau) = \int_{-\infty}^{\tau} d\tau' h(\tau - \tau')C_A(\tau'). \quad (4)$$

By comparing Eqs. (2) and (4) we see that the relation between $E_{in}(t)$ and $E_{out}(t)$ is exactly the same as that between $C_A(\tau)$ and $C_C(\tau)$. That is, in the linear regime, by comparing $C_A(\tau)$ and $C_C(\tau)$ we can see the deformation of light pulses by their passage through the sample.⁸⁻¹⁰

The same Ti:sapphire laser output is guided to the first Michelson interferometer to form a train of two excitation pulses to burn the population grating in the sample. The time separation and the phase relation between the two excitation pulses are controlled by the path-length difference, or the delay time τ_1 , between the two arms of the first Michelson interferometer. Phase locking between the two excitation pulses is indispensable for stable accumulation of the population grating.

If the sample is irradiated by the output beam from the first Michelson interferometer, an infinite series of two-pulse excitations occurs, and the population grating accumulates in the sample. The input light pulse to the sample in the signal arm of the second Michelson interferometer is deformed not only by the initial absorption but also by the burned population grating in the sample to emit an echo pulse as a FID signal, and thus this input pulse is the last excitation pulse for echo emission. The waveform of the last excitation pulse and the echo pulse can be observed by the second Michelson interferometer as a cross-correlation interferogram between input light $E_{in}(t)$ and output light $E_{out}(t)$ from the sample.

By Fourier transformation of Eq. (2) we obtain

$$E_{out}(\omega) = h(\omega)E_{in}(\omega), \quad (5)$$

where $E_{in}(\omega)$ and $E_{out}(\omega)$ are the Fourier transforms of $E_{in}(t)$ and $E_{out}(t)$, respectively, and $h(\omega)$, which is called the complex transmission coefficient, is the Fourier transform of the impulse-response function $h(t)$. The Fourier transformation of Eq. (4) yields a relation similar to Eq. (5):

$$C_C(\omega) = h(\omega)C_A(\omega), \quad (6)$$

where $C_A(\omega)$ and $C_C(\omega)$ are the Fourier transforms of autocorrelation $C_A(\tau)$ and cross correlation $C_C(\tau)$, respectively. By using these relations we can obtain the complex transmission coefficient from the measured autocorrelation and cross-correlation interferograms.

The sample that we used was 3,3'-diethylthiatricarbocyanine iodide (DTTCI) doped in a 100- μm thick poly(vinyl alcohol) (PVA) film, and it was kept at a temperature of 10 K in a cryostat. The absorption spectrum of the sample and the spectrum of the mode-locked Ti:sapphire laser are shown in Fig. 2. The laser light excites the low-frequency band edge of the S_0 -to- S_1 transition of DTTCI dye molecules where the 0-0 transition is located. The average power of the beam for a train of two-pulse excitation and the beam for the last excitation pulse and the reference pulse are 1.5 mW and 40 μW , respectively. The spot sizes of all the incident beams were 1 ϕ at the sample.

3. RESULTS AND DISCUSSION

Figure 3 shows the cross-correlation interferograms between input light $E_{in}(t)$ and output light $E_{out}(t)$ from the sample measured with the second Michelson interferometer with the two-pulse excitation beam off [curve (a)] and on [curve (b)]. In curve (b), where the population grating is burned in the sample, we can clearly see an echo pulse, which is emitted at a time $\tau_1 = 1000$ fs after the last excitation pulse. Delay time τ_1 is exactly the same as the

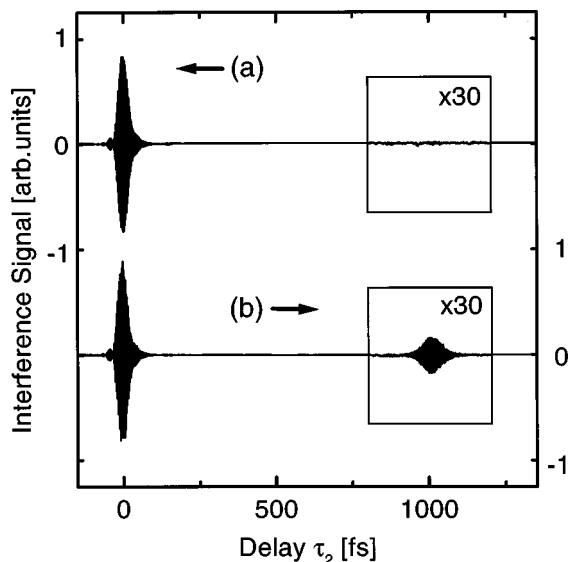


Fig. 3. Cross-correlation interferograms between input light $E_{in}(t)$ and output light $E_{out}(t)$ from the sample measured with the second Michelson interferometer when the two-pulse excitation is (a) off and (b) on.

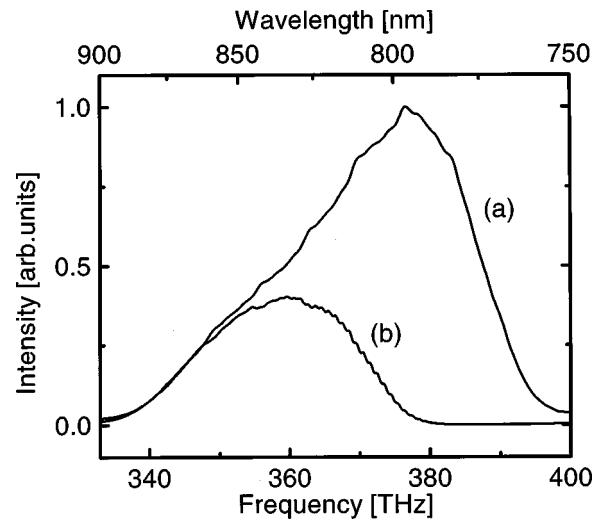


Fig. 4. Power spectra of (a) input light and (b) output light through the burned sample obtained from Fourier analysis of the measured autocorrelation and cross-correlation interferograms.

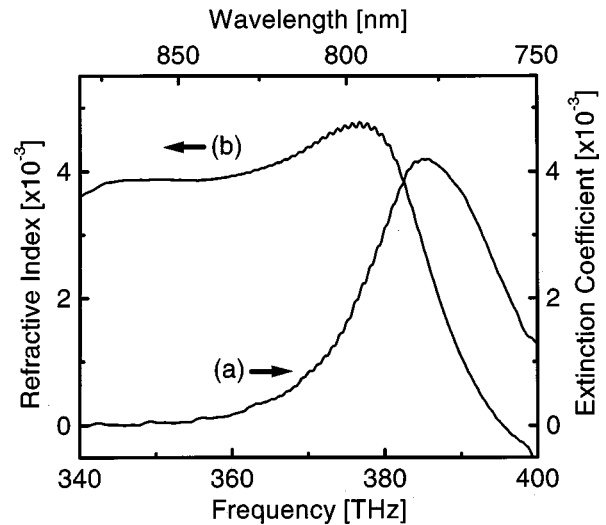


Fig. 5. (a) Extinction coefficient and (b) refractive index of the burned sample obtained from Fourier analysis of the measured autocorrelation and cross-correlation interferograms.

time separation between the two excitation pulses formed by the first Michelson interferometer. Because homogeneous phase decay time T_2 of the 0-0 transition at 10 K is of the order of 100 ps,¹² the time separation between the first and the second excitation pulses, $\tau_1 = 1000$ fs = 1 ps, is well within the homogeneous phase decay time.

The power spectra of the input light and the output light from the sample and the complex transmission coefficient are obtained by Fourier analysis of the measured autocorrelation and cross-correlation interferograms. Curves (a) and (b) of Fig. 4 are the power spectra of the input light and the output light from the burned sample, respectively, and curves (a) and (b) of Fig. 5 show the extinction coefficient and the refractive index, respectively. We can clearly see the modulation in the output

spectrum and the complex transmission coefficient that are due to the burned population grating.

We can extract the effect of the population grating by subtracting the cross-correlation interferograms for the echo pulse on and off, and the interferograms are shown in curve (a) of Fig. 6 for the extinction coefficient and in curve (b) for the refractive index. The modulation frequency, 1 THz, is the inverse of the time separation, $\tau_1 = 1$ ps, between the first and the second excitation pulses. The modulation of the extinction coefficient and of the refractive index is shown in detail in Fig. 7. The modulation amplitudes of the two cases are almost the same, but the phase of the modulation of the extinction coefficient is $\pi/2$ ahead of the refractive index, as expected from the Kramers–Kronig relation.

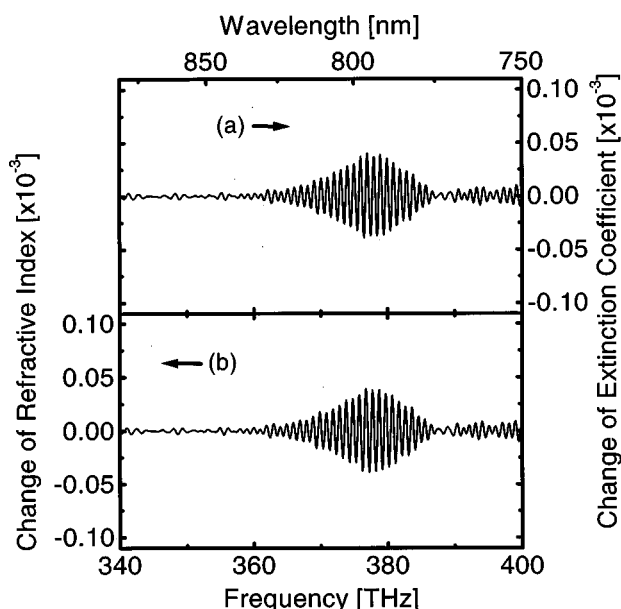


Fig. 6. Changes in (a) the extinction coefficient and (b) the refractive index caused by the population grating burned in the sample.

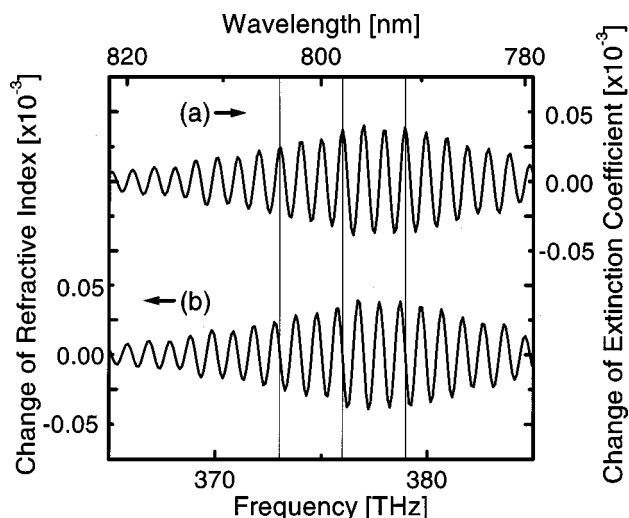


Fig. 7. Changes in (a) the extinction coefficient and (b) the refractive index caused by the population grating burned in the sample. The phase of the modulation of extinction coefficient is $\pi/2$ ahead of that of the refractive index.

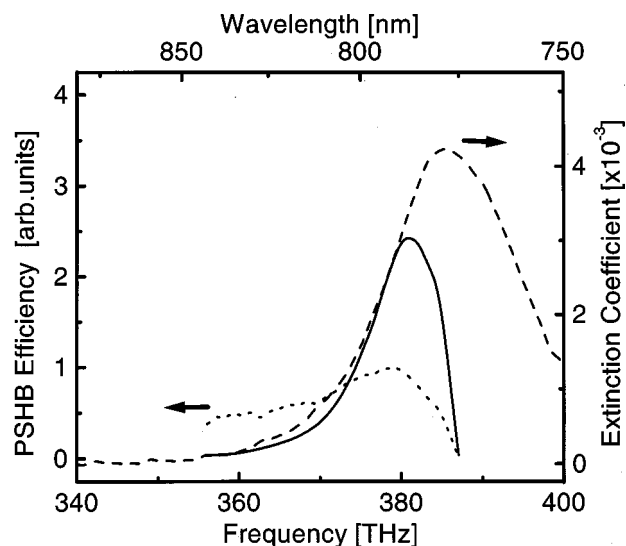


Fig. 8. Initial extinction coefficient of the DTTCI-doped PVA film (dashed curve) and quantum efficiency of PSHB (dotted curve). The solid curve is the product of the extinction coefficient and the quantum efficiency that represents the frequency distribution of dye molecules that is efficient for PSHB.

In dye-doped polymer films at low temperatures, sharp persistent spectral holes are burned by the irradiation of monochromatic light, which is resonant on the 0–0 transition. If the dye molecules are excited to a vibrationally excited state, however, fast vibrational relaxation occurs and results in a wide, small hole. The population grating in the present experiment is made by persistent spectral hole burning (PSHB). We calculated the frequency dependence of the PSBH quantum efficiency by dividing the depth of the population grating by the absorbed photon number, as shown in Fig. 8 by the dotted curve; the dashed curve shows the initial extinction coefficient of the dye-doped polymer film. The product of the quantum efficiency and the extinction coefficient gives the frequency distribution of dye molecules that is efficient for PSBH, as shown by the solid curve in Fig. 8. The effective frequency distribution for PSBH is located on the low-frequency side of the absorption band and coincides with the location of the expected 0–0 transition between S_0 and S_1 levels. The PSBH inefficient absorption on the higher-frequency side of the absorption band is considered to be due to the transitions to the vibrationally excited states. If we assume that the PSBH efficiency distribution represents the inhomogeneous frequency distribution of the 0–0 transition, the inhomogeneous width is estimated to be 10 THz. The reason for the gradual decrease of PSBH efficiency at frequencies lower than ~ 380 THz is not clear at present, but it might be the hole refilling effect of hole burning on the higher-frequency side.¹³

4. CONCLUSION

We have observed the waveform of accumulated photon echoes in a DTTCI-doped PVA film by using a Michelson-type interferometer. By Fourier analysis of the measured interferograms we obtained detailed shapes of the population grating and of the phase grating burned in the

sample. From a frequency distribution of the dye molecules that is efficient for PSHB we estimated the inhomogeneous frequency distribution of the 0–0 transition from S_0 to S_1 levels of DTTCI in PVA. This interferometric method may be applied to other kinds of phase-sensitive ultrafast nonlinear spectroscopy.

ACKNOWLEDGMENTS

This research was supported in part by a grant-in-aid for scientific research (B) from the Ministry of Education, Science, Sports and Culture, Japan.

H. Nakatsuka's e-mail address is nakatsuk@bk.tsukuba.ac.jp.

REFERENCES

1. K. Duppen and D. A. Wiersma, "Picosecond multiple-pulse experiments involving spatial and frequency gratings: a unifying nonperturbation approach," *J. Opt. Soc. Am. B* **3**, 614–621 (1986).
2. W. H. Hesselink and D. A. Wiersma, "Picosecond photon echoes stimulated from an accumulated grating," *Phys. Rev. Lett.* **43**, 1991–1994 (1979).
3. J.-Y. Bibot, M.-A. Mycek, S. Weiss, R. G. Ulbrich, and D. S. Chemla, "Instantaneous frequency dynamics of coherent wave in semiconductor quantum wells," *Phys. Rev. Lett.* **70**, 3307–3310 (1993).
4. M. S. Pshenichnikov, K. Duppen, and D. A. Wiersma, "Time-resolved femtosecond photon echo probes bimodal solvent dynamics," *Phys. Rev. Lett.* **74**, 674–677 (1995).
5. J.-P. Likforman, M. Joffre, and V. T. Mieg, "Measurement of photon echoes by use of femtosecond Fourier-transform spectral interferometry," *Opt. Lett.* **22**, 1104–1106 (1997).
6. M. F. Emade, W. P. de Boeij, M. S. Pshenichnikov, and D. A. Wiersma, "Spectral interferometry as an alternative to time-domain heterodyning," *Opt. Lett.* **22**, 1338–1340 (1997).
7. S. M. Gallagher, A. W. Albrecht, J. D. Hybl, B. L. Landin, B. Rajaram, and D. M. Jones, "Heterodyne detection of the complete electric field of femtosecond four-wave mixing signal," *J. Opt. Soc. Am. B* **15**, 2338–2345 (1998).
8. N. Tsurumachi, T. Fuji, S. Kawato, T. Hattori, and H. Nakatsuka, "Interferometric observation of femtosecond free induction decay," *Opt. Lett.* **19**, 1867–1869 (1994).
9. T. Fuji, M. Miyata, S. Kawato, T. Hattori, and H. Nakatsuka, "Linear propagation of light investigated with a white-light Michelson interferometer," *J. Opt. Soc. Am. B* **14**, 1074–1078 (1997).
10. T. Fuji, M. Arakawa, T. Hattori, and H. Nakatsuka, "A white-light Michelson interferometer in the visible and near infrared regions," *Rev. Sci. Instrum.* **69**, 2854–2858 (1998).
11. N. F. Scherer, R. J. Carlson, A. Matro, M. Du, A. J. Ruggiero, V. Romero-Rochin, J. A. Cina, G. R. Fleming, and S. A. Rice, "Fluorescence-detected wave packet interferometry: time resolved molecular spectroscopy with sequences of femtosecond phase-locked pulse," *J. Chem. Phys.* **95**, 1487–1511 (1991).
12. S. Uemura, M. Okada, A. Wakamiya, and H. Nakatsuka, "Host-structure-dependent non-Lorentzian persistent-hole shapes in organic glasses," *Phys. Rev. B* **46**, 10,641–10,649 (1992).
13. L. Shu and G. J. Small, "Dispersive kinetics of nonphotochemical hole burning and spontaneous hole filling: Cresyl Violet in polyvinyl films," *J. Opt. Soc. Am. B* **9**, 733–737 (1992).